

Novel composites materials from functionalized polymers and silver coated titanium oxide capable for calcium phosphate induction, control of orthopedic biofilm infections: an “in vitro” study

M. Tyllianakis · E. Dalas · M. Christofidou · J. K. Kallitsis · A. Chrissanthopoulos · P. G. Koutsoukos · C. Bartzavali · N. Gourdoupi · K. Papadimitriou · E. K. Oikonomou · S. N. Yannopoulos · D. Sevastos

Received: 15 January 2009 / Accepted: 26 April 2010 / Published online: 29 May 2010
© Springer Science+Business Media, LLC 2010

Abstract Three copolymers containing the functional groups P=O, S=O and C=O were prepared, and upon the introduction in calcium phosphate aqueous solutions at physiological conditions, “in vitro” were induced the precipitation of calcium phosphate crystals. The investigation of the crystal growth process was done at constant supersaturation. It is suggested that the negative end of the above

functional groups acts as the active site for nucleation of the inorganic phase. In order to obtain the copolymer further antimicrobial activity, titania (TiO₂) nanocrystals were incorporated in the polymer matrix after silver coverage by UV radiation. The antimicrobial resistance of the composite material (copolymer-titania/Ag) was tested against *Staphylococcus epidermidis* (SEM), *Staphylococcus aureus* (SAM), *Candida parapsilosis* (CAM) and *Pseudomonas aeruginosa* (PAM), microorganisms, using cut parts of “ π -plate” that covered with the above mentioned composite. The antimicrobial effect increased as the size of the nanocrystals TiO₂/Ag decreased, the maximum achieved with the third polymer that contained also quaternary ammonium groups.

M. Tyllianakis (✉)
Department of Orthopaedic, Patras University Hospital,
26504 Rio, Patras, Greece
e-mail: mintylli@med.upatras.gr

E. Dalas · J. K. Kallitsis · A. Chrissanthopoulos ·
K. Papadimitriou · E. K. Oikonomou · D. Sevastos
Department of Chemistry, University of Patras,
26504 Rio, Patras, Greece
e-mail: vdal@chemistry.upatras.gr

M. Christofidou · C. Bartzavali
Department of Microbiology, School of Medicine,
University of Patras, 26504 Rio, Patras, Greece

A. Chrissanthopoulos
Department of Material Science, University of Patras,
26504 Rio, Patras, Greece

P. G. Koutsoukos
Department of Chemical Engineering, University
of Patras, 26504 Rio, Patras, Greece

J. K. Kallitsis · P. G. Koutsoukos · E. K. Oikonomou ·
S. N. Yannopoulos
Foundation for Research and Technology Hellas, Institute
of Chemical Engineering and High Temperature Chemical
Processes, FORTH/ICE-HT, P.O. Box 1414, 26504 Rio,
Patras, Greece

N. Gourdoupi
Advent Technologies S.A. Patras Science Park,
Stadiou Street, Patras 26504, Greece

1 Introduction

Joint replacements and fracture osteosynthesis are among the most common surgical procedures. Total hip and knee arthroplasties in the USA account for more than 500.000 operations each year [1–3] thus creating an enormous population of patients with implanted orthopaedic materials. Although the risk of infection in these patients is low (0.5–5% for joint replacements), the consequences may be very serious, because sometimes simple debridement procedures with retention of the prosthesis and antibiotic administration are not enough [4] and the implant has to be removed and replaced or the joint to be fused in order to eradicate the infection [5]. These measures greatly affect both the patient and the health system [6].

In order to prevent infection pre- and perioperative aseptic measures have been improved, operating techniques have been refined and antibiotic prophylaxis is widely used. Furthermore much attention has been focused

on the pathogenesis of the infection, especially those associated to implant materials, as the latter have been found to be colonized by biofilms, which are composed of microcolonies enclosed in a highly hydrated polymeric matrix surrounded by interstitial voids. Within biofilms microorganisms develop into organized communities and are protected from environmental influences including host immune responses and normal levels of conventional antimicrobial agents [7]. In vitro data indicate that microorganisms in biofilms are substantially more resistant to killing by antimicrobial agents than are planktonic bacteria, the resistance being increased as the biofilm ages.

Inhibition of microbial adherence is one of the strategies for controlling biofilms. Ribonucleic acid III-inhibiting peptide seems to be synergistic with conventional antimicrobial agents [8], application of ultrasound, [9–12] low electric current combined with antimicrobial agent [13–20] and use of various chemicals are some of the measures that have been used to avert biofilm adherence.

Hydroxyapatite ($\text{Ca}_5(\text{PO}_4)_3\text{OH}$, HAP) is considered as the model compound for the inorganic constituent of bone and teeth. Blood serum may be considered as an aqueous solution supersaturated to a number of calcium phosphates [21]. Due, however, to the presence of macromolecules such as proteins, enzymes etc. in biological fluids, extensive complexation of the free calcium takes place, thus reducing the actual supersaturation [22]. As a result, it has been recommended that “in vitro” experiments should be conducted at low supersaturations [23–26] by the constant composition technique.

The aim of the present work is (a) the development of a coating (a functionalized polymer) outstanding mechanical and chemical resistance as well as the capability of inducing calcium phosphate nucleation (HAP) and subsequent growth. (b) Prevent the formation of microbial biofilms and further infections of the implant area.

2 Experimental

2.1 Preparation of the functionalized copolymers for the coverage of the implanted metals

The chemical structure of the polymer 1, PP_yPO (poly (2,5-biphenyloxy pyridiny phosphin oxide)) is shown in Table 1 and synthesized as described in detailed in the literature [27]. The polymer is soluble in common organic solvents such as CHCl_3 , THF, DMF allowing its GPC and $^1\text{H-NMR}$ characterization. GPC measurements using CHCl_3 as eluent versus PS standard calibration revealed a molecular weight of $M_n = 30000$, $M_w = 67000$ and $I = 2.2$.

The functional group acting as nucleator for the calcium phosphate is the $-\text{P}=\text{O}$ as well defined in the literature [26]

and the polymer was used as substrate for the calcification experiments structural characterization using $^1\text{H-NMR}$ gave peaks at: $^1\text{H NMR (CDCl}_3)$: 8.88 (s, 1H), 8.05 (d, 2H), 7.92 (d, 1H), 7.77 (d, 1H), 7.47–7.71 (three m, 11H), 7.16 (d, 4H), 7.1 (d, 4H).

For the preparation of polymer 2 (Table 1), PP_y(80)-coPO, a synthesis procedure of a previous work was also followed [28]. After the synthesis, the polymer was characterized by GPC and $^1\text{H-NMR}$. GPC measurements using CHCl_3 as eluent versus PS standard calibration revealed a molecular weight of $M_n = 16000$, $M_w = 31000$ and $I = 1.93$. $^1\text{H-NMR}$ gave peaks at: $^1\text{H NMR (CDCl}_3)$: 8.88 (s, 1H), 8.05 (d, 2H), 7.92 (d, 1H), 7.77 (d, 1H), 7.47–7.71 (three m, 11H), 7.16 (d, 4H), 7.1 (d, 4H).

For the polymer 3 (Table 1) the synthesis was based on the preparation of PSSNa-b-PMMA block copolymer according to our previous published procedure [29]. This synthesis, was based on the polymerization of MMA through ATRP using a macroinitiator of PSSNa (synthesized also through ATRP). The PSSNa-b-PMMA copolymer is soluble in water and DMSO. The molar mass of the copolymer is determined by $^1\text{H-NMR}$ to be about 15000 as it could not easily be determined by GPC. The success of the polymerization was confirmed by $^1\text{H-NMR}$ in d_6 -DMSO and FT-IR. According to $^1\text{H-NMR}$, the composition was estimated to 40% mol of PSSNa and 60% mol of PMMA. The quaternized ammonium groups were introduced in the polymer through an ion exchange procedure. In particular, the PSSNa-b-PMMA block copolymer was dissolved in water and a surfactant (hexadecyl trimethyl ammonium bromide) aqueous solution was added in excess. The polymer was precipitated and washed with water several times and it was dried in a vacuum oven at 60°C. The $^1\text{H-NMR}$ of the product is presented in Fig. 1 with the respective assignment of the peaks.

The polymer 3 acts as nucleator for calcium phosphate (HAP) through the functional groups $\text{S}=\text{O}$ and $\text{C}=\text{O}$, as well as antimicrobial agent through the $\text{N}^+(\text{CH}_3)_3\text{C}_{16}\text{H}_{33}$ group. The precursor of polymer 3 is an amphiphilic copolymer which is soluble in water. However, when quaternized ammonium groups are introduced to the polymer through ion exchange procedure, the polymer becomes hydrophobic as are polymers 1 and 2 in order to avoid migration of the polymer in aqueous environment. The reason of using such different polymers is to combine the film forming ability of polymer 1 and 2 with the hydroxyapatite precipitation ability of the same polymers and the biocidal activation of the copolymer 3 and silver nanoparticles resulting in robust composite which is used as coating in order to prevent biofilm formation.

Finally seed crystals of calcium phosphate (HAP) were synthesized [30, 31] for the control calcification experiments.

Characterization of all materials prepared was performed using: (a) ^1H , ^{13}C NMR spectroscopy on a Bruker Advance

Table 1 Polymers used for calcium phosphate induction

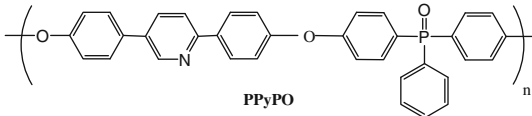
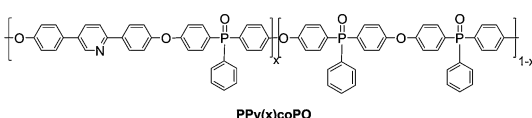
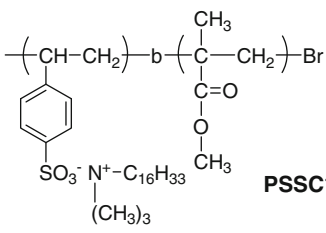
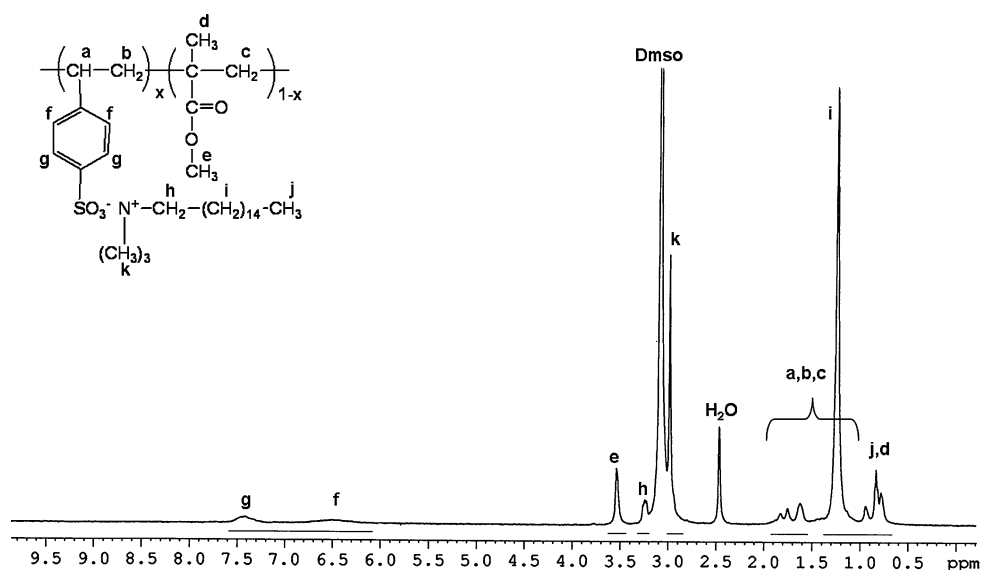
No	Structure	SA (m ² g ⁻¹)	Refs.
1	 <p style="text-align: center;">PPyPO</p>	0.015	[27]
2	 <p style="text-align: center;">PPy(x)coPO</p>	11.4	[28]
3	 <p style="text-align: center;">PSSC16-b-PMMA</p>	8.6	[29]
4	HAP (calcium phosphate)	34.6	[30]

Fig. 1 ¹H NMR of polymer 3

DPX400 and 100 MHz, with deuterated CHCl₃ or DMSO; (b) gel permeation chromatography (GPC) using a Polymer Lab chromatograph equipped with two Ultra Styragel columns (10⁴, 500 Å) and a UV detector (254 nm) and using CHCl₃ as eluent; (c) thermogravimetric analysis (TGA) was

performed at a DuPont 990 thermal analyzer; (d) Fourier transform-infrared (FT-IR) spectroscopy (Perkin-Elmer 16-PC); (e) X-ray diffraction analysis (Phillips PW 1830/1840) and (f) scanning electron microscopy (LEO SUPRA 35VP) equipped with a Bruker EDX microanalysis.

2.2 Calcification experiments “in vitro”

The experiments were done in metastable supersaturated solutions at concentrations appropriate for ensuring stability for long time periods by constant supersaturation approach [32]. All experiments were done at 25°C in a 0.250 dm³ Pyrex glass double walled vessel thermostated at 25 ± 0.1°C by circulating water. More details on this procedure have been described in the literature [24–26, 32, 33]. During the course of reaction, samples were withdrawn so as to keep the total volume approximately constant, filtered through a membrane filter (0.2 µm, Gelman, Gellulose Nitrate), and the filtrates were analyzed for calcium and phosphate. The solid phases on the filters were analyzed by powder X-ray diffraction, FT-IR spectroscopy, specific surface area (multiple point B.E.T. Perkin Elmer Model 212D sorptometer) and thermogravimetric analysis TGA. The experimental conditions are summarized in Table 2 and the rates of HAP formation were taken from the plots of titrant addition as a function of time. The reproducibility of the measured rates was ±4%, a mean of five experiments. Finally the stoichiometric ratio Ca:P experimentally determined in the solid phases was 1.67 ± 0.01.

Table 2 Crystal growth of HAP on functionalized polymers at sustained supersaturation

Substrate or inhibitor	10 ⁻⁴ Ca _t (mol dm ⁻³)	ΔG _{HAP} (kJ mol ⁻¹)	10 ⁻⁹ R _{HAP} (mol min ⁻¹ m ⁻²)
HAP seed crystals	5.0	-3.5	97.3
HAP	4.0	-3.0	64.1
HAP	3.5	-2.7	53.8
HAP	3.0	-2.0	31.6
HAP	2.5	-1.5	22.6
Polymer 1	5.0	-3.5	4.6
Polymer 1	4.0	-3.0	4.3
Polymer 1	3.5	-2.7	2.1
Polymer 1	3.0	-2.0	1.4
Polymer 1	2.5	-1.5	1.0
Polymer 2	5.0	-3.5	14.7
Polymer 2	4.0	-3.0	13.7
Polymer 2	3.5	-2.7	6.7
Polymer 2	3.0	-2.0	4.5
Polymer 2	2.5	-1.5	3.2
Polymer 3	5.0	-3.5	8.1
Polymer 3	4.0	-3.0	7.5
Polymer 3	3.5	-2.7	3.7
Polymer 3	3.0	-2.0	2.5
Polymer 3	2.5	-1.5	1.8

Conditions 37°C, pH 7.40, (total calcium Ca_t/total phosphate P_t) = 1.67, 0.15 M NaCl, SSA of HAP = 34.6 m²/g

2.3 Preparation and characterization of the biofilm resistant and antimicrobial factor

Titanium and titanium alloys are well accepted as bio-compatible implants in orthopaedic surgery and generally are surface coated with TiO₂. In this work two types of titania nanocrystals were used. Type I was purchased from Degussa, P25, SA = 50 m²/g, particle diameter 30 nm and isoelectric point variable from pH 4.4 to 6.4. Type II was synthesized by a sol-gel method described elsewhere [34], SA = 114 m²/g and particle diameter 6.4 nm. The TiO₂ nanocrystals were suspended in DMSO (dimethylsulfoxide) along with silver nitrate (Degussa, proanalysis) 2% w/v and the suspension was illuminated by a UV pencil lamp, Hach 20823 at 240 nm. As a result after 5 min illumination the titania nanoparticles were covered with Ag. Titania is photocatalytic because it is a semiconductor, meaning that a moderate amount of energy is needed to lift an electron from the mineral's so-called valence band or filled energy levels across what is known as a band gap (composed of forbidden energy levels) into the empty “conduction band” where electrons can flow and elemental silver coated on the surface of the nanocrystals by the reaction



In Fig. 2 the particle size distributions for the two suspensions are shown before and after silver deposition. They were constructed with the DLS method measuring the

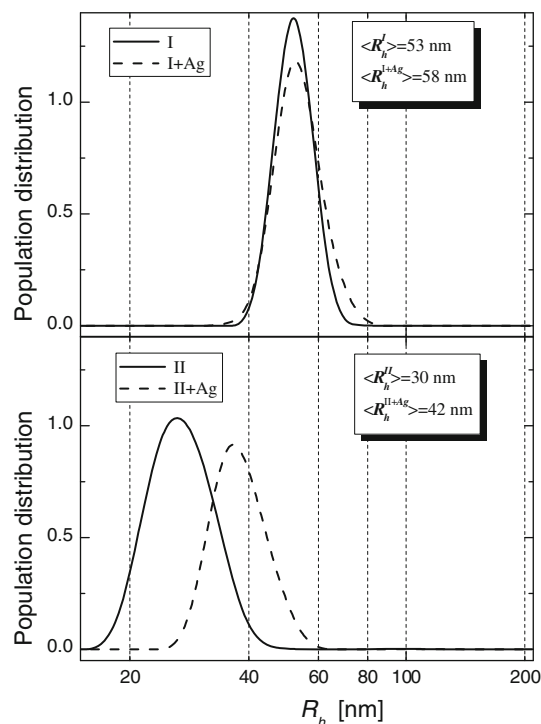


Fig. 2 Particle size distribution of titania nanocrystals I, II before and after silver coverage

normalized intensity-time-correlation functions over a broad time scale (from 10^{-8} s to 10^4 s) using a full multiple tau digital correlator (ALV-5000/FAST) with 280 channels spaced quasi-logarithmically [35].

2.4 Antimicrobial resistance—laboratory testing of microorganisms in biofilms

Cut parts (CP) approximately 1 cm each of “ π -plate” (Synthes-Switzerland) which is used for osteosynthesis of distal radius fractures. The polymer 4% w/v were dissolved in the titania suspensions in DMSO (titania nanoparticles were covered by silver first) and this solution used for painting the cut parts of the “ π -plate” resulting in a composite polymer coverage 50 μ m approximately after DMSO evaporation in an oven at 50°C.

Pseudomonas aeruginosa (PAM), *Staphylococcus aureus* (SAM), *Staphylococcus epidermidis* (SEM) and *Candida parapsilosis* (CAM), were clinical isolates from the collection of the Department of Medical Microbiology—Patras—Greece. Vitek system (bioMerieux) was used for species identification whereas all isolates were tested and were characterized as biofilm producers.

The ability of such microorganisms to organize into biofilms was demonstrated by a modified test using crystal violet stain. Clinical isolates were cultivated for 24 h in Brain Heart Infusion Broth (BHIB, Oxoid), in microtitration plate wells. After incubation the BHIB containing free planktonic cells was drained. Each well was then stained with 1% crystal violet, rinsed with distilled water, dried and visually evaluated for the presence of biofilm [36].

Four series of five test tubes, containing 5 ml each, Tryptic Soy Broth (TSB, Oxoid), were prepared. The five tests tubes of each series were inoculated with five colonies of each microorganism for each tube. A tube without inoculum in each series, served as a negative control, included.

In the first series, CP with the polymer composite coverage (CPP) was separately and aseptically placed, one in each test tube. The same was done in the second series while CP were without polymer composite coverage. We repeated the same in the third and fourth series of tubes.

The four series of tubes were then incubated for 48 h at 37°C in a shaking incubator. Evidence of microbial growth according to gross visual media opacity was evaluated at 48 h.

CPP from the first series of tubes and CP from the second series separately and aseptically placed in sterile tubes and rinsed with 50 ml sterile normal saline (0.9% NaCl). Free planktonic cells were removed and then the CPP and CP placed once again in tubes with 5 ml BHIB and were vortexing vigorously. Quantitative microbial cultures on blood agar (Oxoid) were done by 1 μ l of BHIB

suspension and the numbers of cultivated microorganisms were evaluated.

CPP from the third series of tubes and CP from the fourth series, separately and aseptically placed in empty sterile tubes and examined using the scanning electron microscopy [37].

Staphylococcus (*S. aureus*, *S. epidermidis*), *Pseudomonas* and *Candida* spp are genus of bacteria and fungi which are characterized as biofilm producers [36, 37]. These strains are nosocomial ones. *S. aureus*, *S. epidermidis* and *P. aeruginosa* were isolated from different patients with bacteremia whereas *Candida parapsilosis* was isolated from a case of Candidemia. The strains were identified by subculture and biochemical tests. *S. aureus* is a MRSA strain, *S. epidermidis* is a MRSE strain whereas, *P. aeruginosa* is a multidrug resistant strain. Biofilm production in these strains was tested by modified test using crystal violet stain [36].

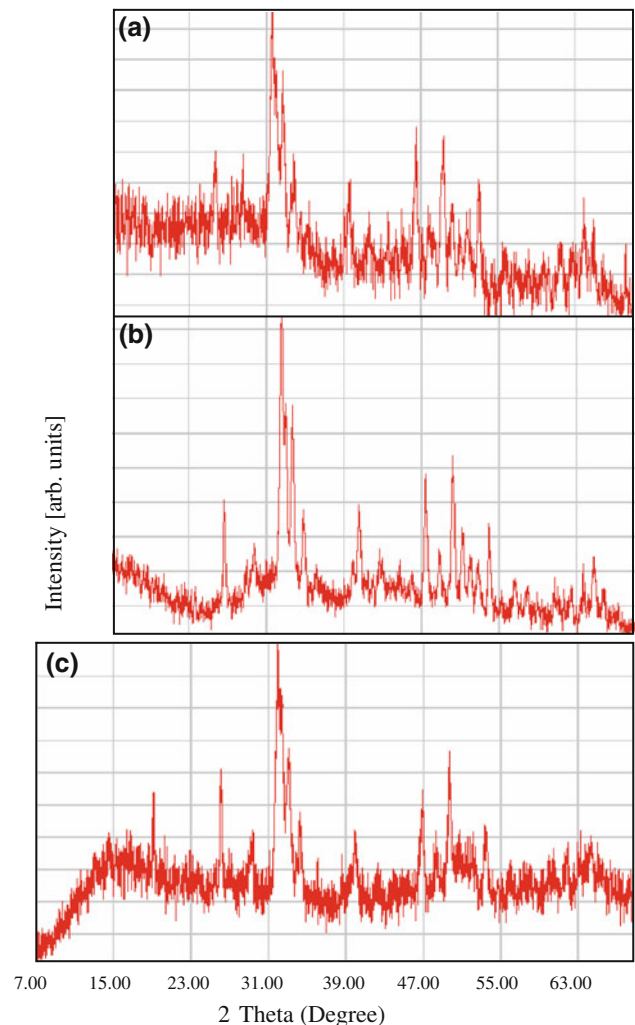


Fig. 3 X-ray diffraction analysis of HAP grown on: **a** polymer 1; **b** polymer 2; **c** polymer 3

3 Results

In all cases of calcification experiments “in vitro” precipitation started on the polymer surface without any appreciable induction time. Spectroscopic examinations by X-ray diffraction [38] exhibits the characteristic reflections for HAP with d-spacing 3.440, 2.817, 2.779, 2.723, 2.265, [hkl (002), (211), (112), (300), (130), respectively] as shown in Fig. 3. Also HAP formation was confirmed from FT-IR spectra (Fig. 4) [39] and elemental analysis $Ca/P = 1.67$. Morphological examination of the precipitated solid revealed the formation of calcium phosphate (HAP) as shown in Fig. 5. The experimental conditions are summarized in Table 2. The solution speciation in all experiments was calculated from the proton dissociation and ion pair formation constants for calcium and phosphate, the mass balance, and electroneutrality conditions by successive approximations for the ionic strength [24]. The driving force of HAP formation is the change in Gibbs free energy, ΔG_{HAP} , for the transfer from the supersaturated solution to equilibrium, $\Delta G_{HAP} = -\frac{R_g T}{9} \ln \Omega_{HAP}$, where R_g is the gas constant, T the absolute temperature, 9 is the

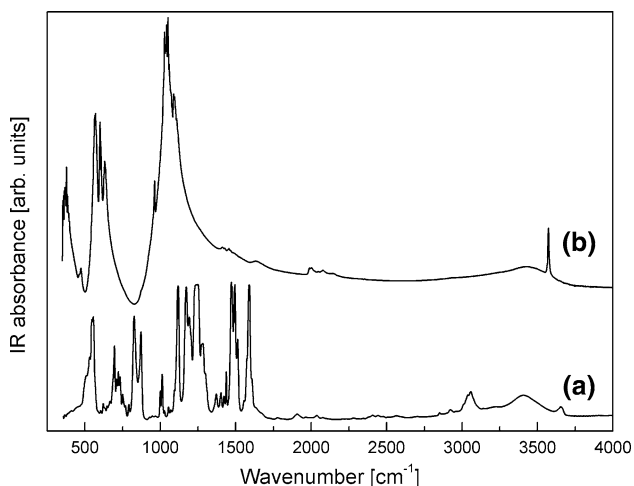


Fig. 4 FT-IR spectra of **a** polymer 3; **b** HAP overgrowth on polymer 3

Fig. 5 Scanning electron micrographs of **a** polymer substrate 1 and **b** calcium phosphate crystals on polymer substrate 1

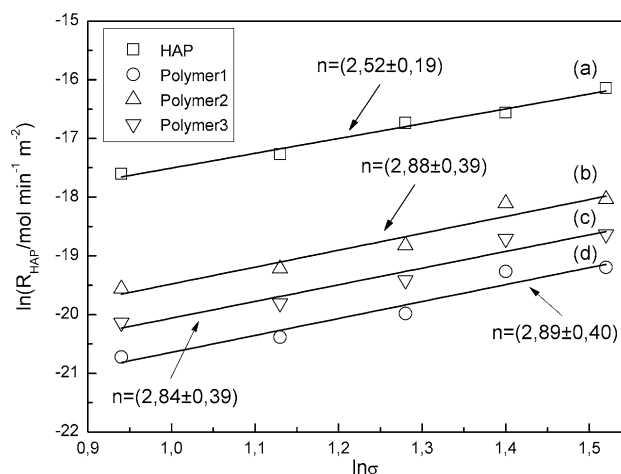
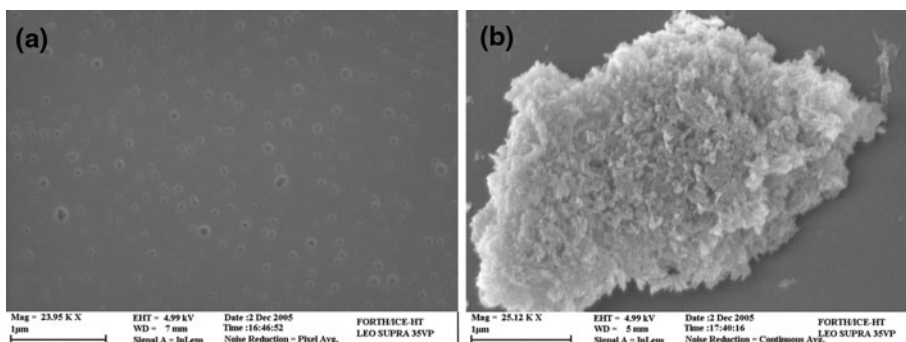


Fig. 6 Rate of HAP precipitation on **a** HAP seed crystals; **b** polymer 2 substrate; **c** polymer 3 substrate; **d** polymer 1 substrate

number of ions and Ω_{HAP} the supersaturation ratio for HAP [26, 31]. The relative solution supersaturation σ , is defined by the Eq. $\sigma_{HAP} = \Omega_{HAP}^{1/9} - 1$ and was found strongly influence the rate of HAP precipitation as may be seen from Table 2 and Fig. 6.

Latest research shows that nanoparticles can penetrate cells with or without leaving holes in the membrane and the process however is intrinsically cytotoxic [40, 41]. The CPP parts showing antimicrobial activity against *Staphylococcus aureus* (SAM), *Staphylococcus epidermidis* (SEM), *Candida parapsilosis* (CAM) and *Pseudomonas aeruginosa* (PAM) depending on the size of titania nanoparticles coated with silver as shown in Table 3 (a mean of five experiments). The above mentioned experimental results were confirmed by scanning electron micrographs (Fig. 7). The biofilms that exhibits increased resistance in antibiotic therapy are present in CPs metallic parts and absent in CPP covered metallic parts by polymer composite and only plaetonic shells are shown for SAM and SEM pathogenic species.

In order to increase the antimicrobial activity of the composite polymer 2 coverage smaller titania particles (Fig. 1) where used also coated with silver and the results

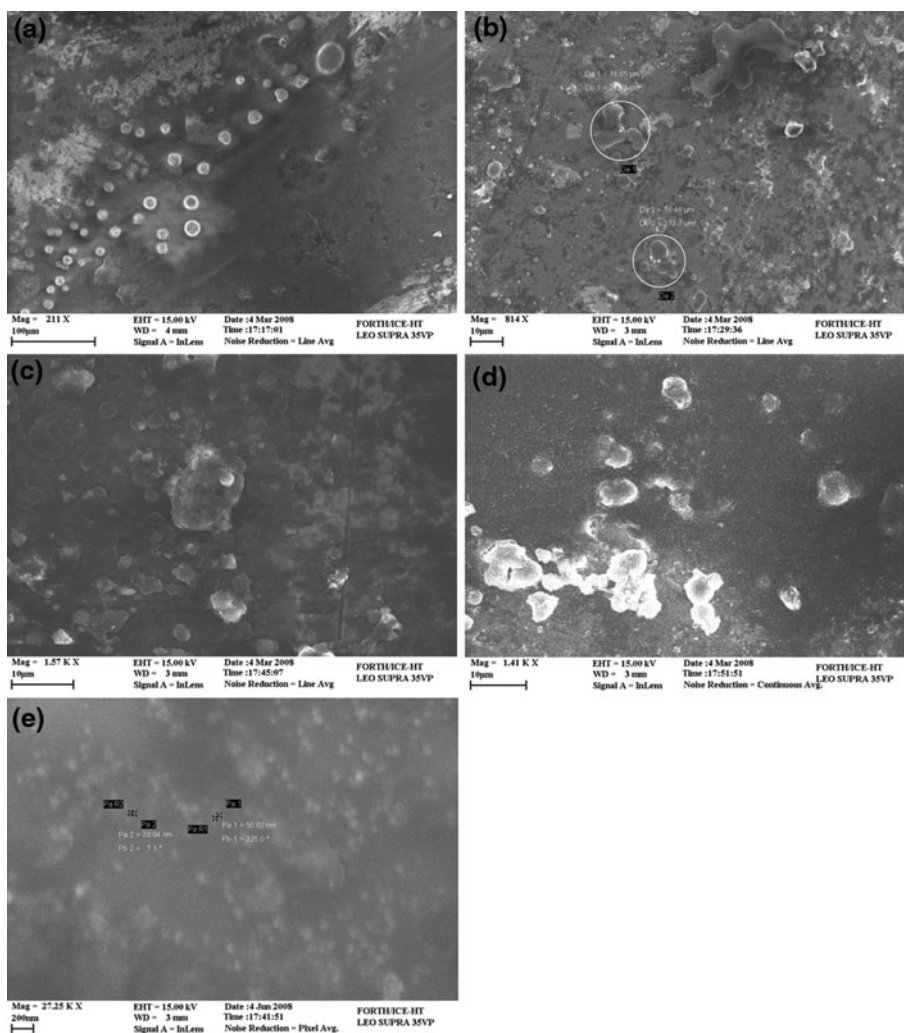
Table 3 The antimicrobial activity of the composite material covered the cut parts (CP) of the “π plates”

Material	SAM	SEM	CAM	PAM	NC
CP	>1000	>1000	60	>1000	(-) Fig. 3
CP/polymer 2 + TiO ₂ I/Ag	50	90	60	100	(-)
CP	400	100000	10	400	(-) Fig. 4
CP/polymer 2 + TiO ₂ II/Ag	(-)	(-)	1	(-)	(-)
CP	>1000	>1000	80	>1000	(-) Fig. 5
CP/polymer 3 + TiO ₂ II/Ag	(-)	(-)	(-)	(-)	(-) +TiO ₂ II

(Table 3) along with scanning electron micrographs (SEM) are shown in Fig. 8. Now the antimicrobial activity of the new material was increased and extended to other new pathogenic species PAM and CAM.

Changing the polymer 2 by polymer 3 (Table 1) containing quaternary ammonium [42] the antimicrobial activity on the CPP parts was increased as shown in Table 3 and Fig. 9.

Fig. 7 Scanning electron micrographs of: **a** SAM biofilms on the metal surface of CP; **b** SAM cells on CP covered with polymer 2 composite, containing TiO₂ II/Ag; **c** SEM biofilms on the metal surface of CP; **d** SEM cells on CP covered with polymer 2 composite containing TiO₂ I/Ag; **e** TiO₂ I particles in the polymer 2 matrix



4 Discussion

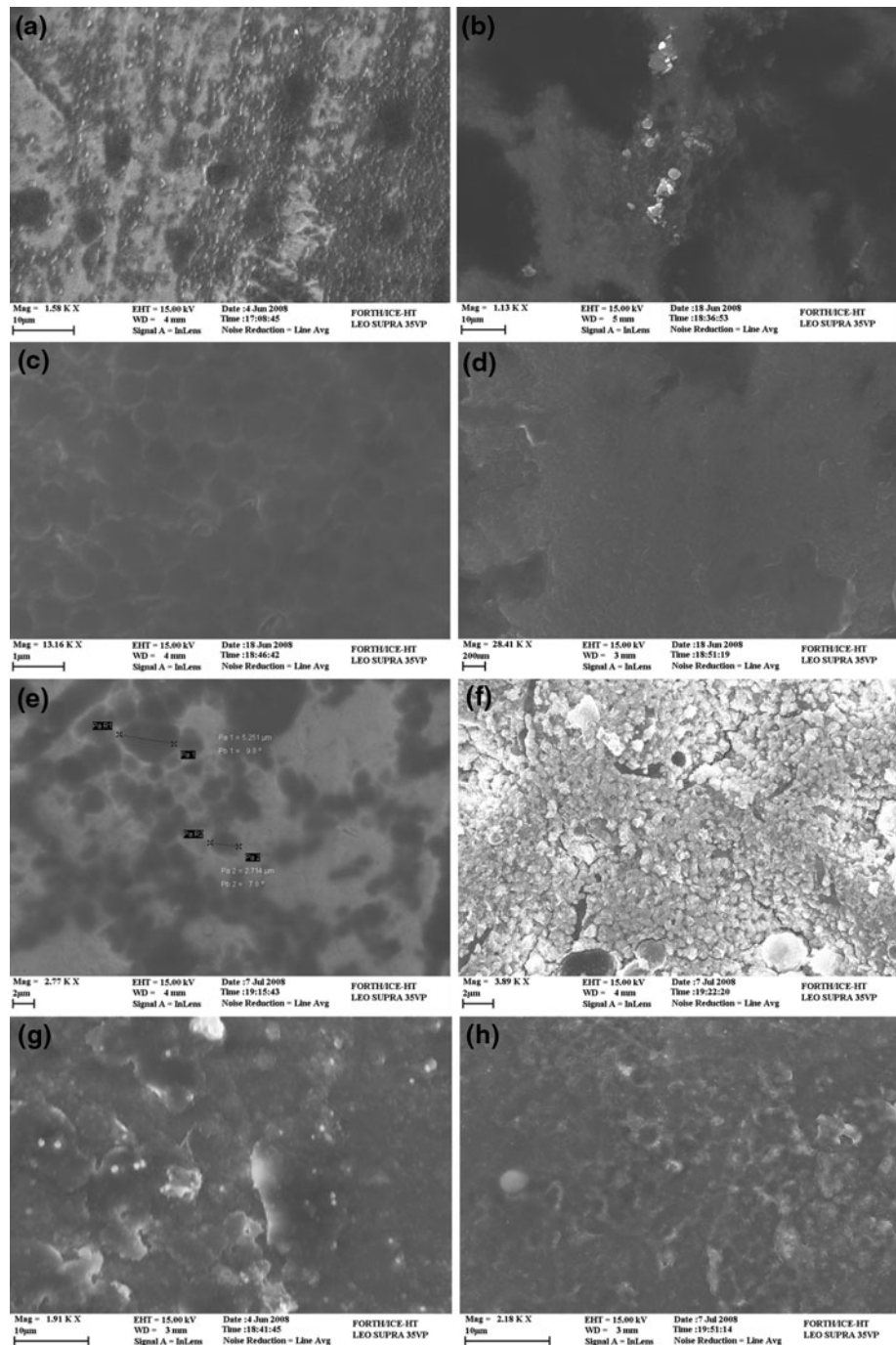
The dependence of the rate of calcium phosphate (HAP) precipitation on polymer 1 as a function of the calcium and phosphate concentration (relative supersaturation, σ_{HAP}) of the working solution “in vitro” conditions (0.15 M NaCl, pH 7.4, 37°C) is shown in Table 2 and described by the equation $R = k \sigma_{HAP}^n$ where $n = 2$ (Fig. 6), indicative of a surface diffusion controlled mechanism [24–26]. Considering the polarity of the P–O bond in which the negative charge is shifted towards the oxygen atom, it may be suggested that the formation of HAP (on polymer 1, 2) was initiated through the interaction of Ca^{2+} ions with the negative end of the P–O bond. Thus, entities such as $Ca \cdots O-P$ were considered as the active sites for the nucleation process [26, 31, 33]. Similar hypothesis is also valid for polymer 3 where the negative end of the C–O or S–O act as nucleation site and the mineralization of biopolymers (collagen fibrils, elastin, fibrin, etc.) [24, 39, 43–45]. The above mechanism was confirmed via computational chemistry calculations using the parametric method 3 (PM3) included in the version

6.0 of MOPAC program package at 310 K [46–48]. This method is based on the neglect of diatomic differential overlap (NDDO) formalism, employs an s-p basis set and does not include d orbitals. It has mean unsigned errors in molecular geometries of 0.036 Å (bond lengths), 3.93° (angles) and 14.9° (torsion angles).

The pathogenesis of many orthopaedic infections is related to the presence of microorganisms in biofilms which are protected from the killing action of antibiotics.

The biofilm can act as a shield for the microorganisms, making it difficult to be reached and destroyed by antibiotic drugs [49]. Many important pathogens SAM (34%), SEM (32%) are in first line among microorganisms and have long been recognized to exhibit always more alarming levels of antibiotic resistance, followed by PAM (8%) [50, 51]. Moreover, bacteria and mycetes CAM (7%) form biofilms on prosthetic surfaces particular by resistance to antimicrobials and tend to survive to aggressive

Fig. 8 Scanning electron micrographs of: **a** SAM biofilms on the metal surface of CP; **b** SAM cells on CP covered with polymer 2 composite, containing TiO₂ I/A_g; **c** SEM biofilms on the metal surface of CP; **d** SEM cells on CP covered with polymer 2 composite containing TiO₂ II/A_g; **e** PAM biofilms on metal surface of CP; **f** PAM cells on CP covered with polymer 2 composite containing TiO₂ II/A_g; **g** CAM biofilms on metal surface of CP; **h** CAM cells on CP covered with polymer 2 composite containing TiO₂ II/A_g



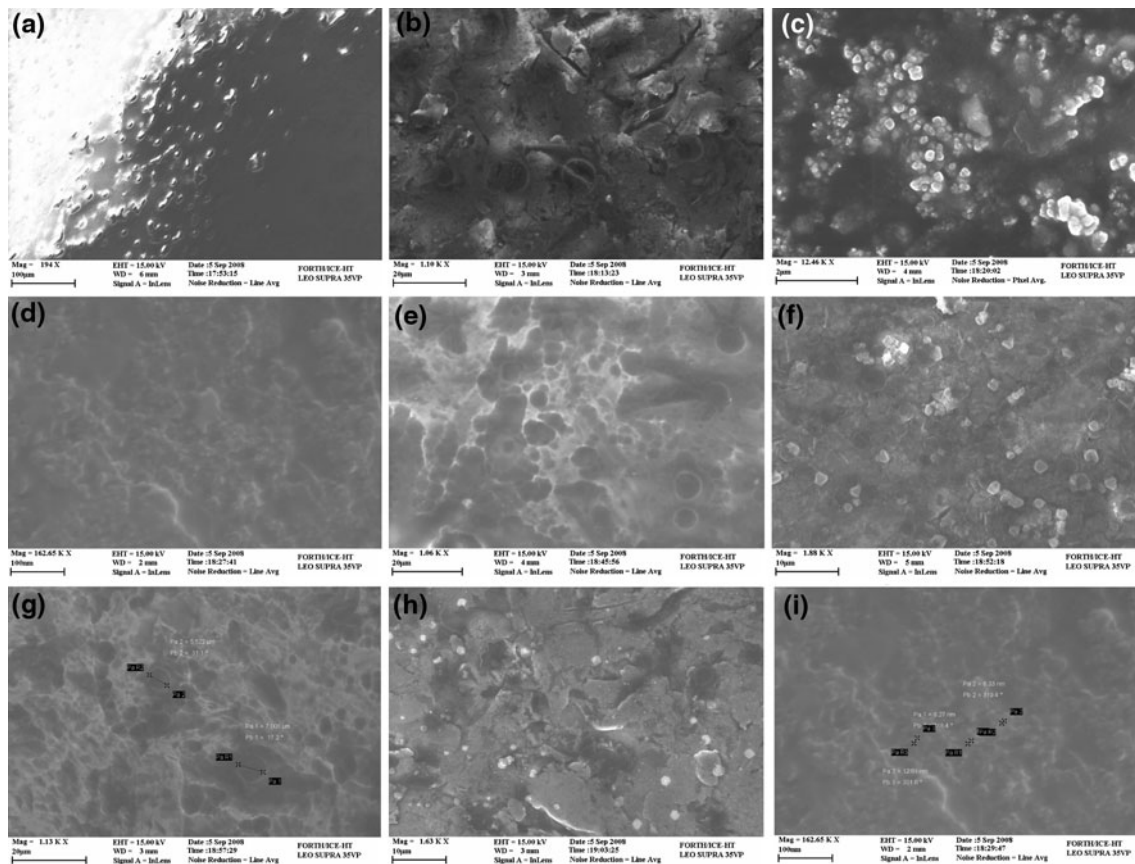


Fig. 9 Scanning electron micrographs of: **a** SAM biofilms on the metal surface of CP; **b** SAM cells on CP covered with polymer 3 composite, containing TiO_2 I I/Ag; **c** SEM biofilms on the metal surface of CP; **d** SEM cells on CP covered with polymer 3 composite containing TiO_2 II/Ag; **e** PAM biofilms on metal surface of CP; **f** PAM

cells on CP covered with polymer 3 composite containing TiO_2 II/Ag; **g** CAM biofilms on metal surface of CP; **h** CAM cells on CP covered with polymer 3 composite containing TiO_2 II/Ag; **i** TiO_2 II particles in the polymer 3 matrix

chemotherapy. This is in accordance to our results where the elimination of CAM biofilms and plactonic cells was achieved by the cooperation of the quaternary ammonium functional groups of polymer 3 and the antimicrobial factor TiO_2 II particles (Fig. 2) covered by silver. Synthetic polymers with quaternary ammonium functional groups showed that they are very potent biosides against microorganisms such as bacteria and mycetes [42]. It is obvious from Table 3 and Fig. 2 that the smaller the size of the titania/silver particles the greater the antimicrobial activity because the penetration of the pathogenic microorganism cells was easier and faster [40, 41], (Fig. 9). Scanning electron micrographs in Fig. 4 where the composite polymer 2 + TiO_2 II/Ag were used for the protection of CP metallic parts are in accordance with the experimental results in Table 3. In other words the composite antimicrobial material is less active in the absence of quaternary ammonium groups, for the CAM microorganisms.

As mentioned in Sect. 2 TiO_2 nanoparticles are semi-conductors and were covered with thin film of metal silver (Fig. 2). These particles possess a strong tunable absorption,

which is determined by the relative core and shell thickness with strong absorbance in the near IR (infrared) where maximal penetration of light through tissue is achieved [51, 52]. Similar nanoparticles composed of a dielectric core (silica, SiO_2) coated with an ultrathin metallic layer (gold, Au) were used by near-IR laser-induced thermal killing of tumor cells [53]. The nanoshells used in this study as a bio-material are composed of elements generally understood to be biocompatible and were stabilized inside the polymer matrix as well as in polymer surface. As a consequence irradiation of the CCP metallic part used as prosthetic material with near-IR (penetrating the solid tissue) resulted in emission of IR radiation in an 100 \AA depth which resulted in elevation of the temperature in this area and thermal elimination of further resistant biofilms or plactonic shells [51–53].

5 Conclusion

The lack of effective antibiotic treatments for infections related to orthopaedic devices and implants demands new

approaches that target biofilms infections on the molecular level. Nanoshells of TiO₂ (titania) particles covered with Ag (silver) incorporated in a polymer matrix are in general biocompatible and demonstrate cytotoxicity against pathogens *Staphylococcus aureus* (SAM), *Staphylococcus epidermidis* (SEM), *Candida parapsilosis* (CAM) and *Pseudomonas aeruginosa* (PAM) cells. This function was strengthened by the quaternary ammonium functional groups added to the polymer matrix. After all, the polymeric matrix due to the P=O, C=O and S=O functional groups initiate the calcium phosphate precipitation on the surface of the implant material.

Acknowledgements Partial support from General Secretariat for Research and Technology, Greece through the program ‘Design and Development of new paints with controlled release of biocides for submarine applications’ PENED 2003, 03ED825, co-financed by E.U.-European Social Fund (75%) and the Greek Ministry of Development-GSRT, is greatly acknowledged.

References

- Brunette DM, Tengvall P, Textor M, Thomsen P, editors. Titanium in medicine. Berlin & Heidelberg, Germany: Springer-Verlag; 2001.
- Leyens C, Peters M, editors. Titanium and titanium alloys: fundamentals and applications. Weinheim, Germany: Wiley-VCH; 2003.
- Textor M, Sitting C, Frauchiger VM, Tosatti SGP, Brunette DM. In: Brunette DM, Tengvall P, Textor M, Thomsen P, editors. Titanium in medicine. Berlin & Heidelberg, Germany: Springer-Verlag; 2001. p. 171–230.
- Brunette DM, Kenner GS, Gould TRL. Grooved titanium surfaces orient growth and migration of cells from human gingival explants. *J Dent Res*. 1983;62:1045–8.
- Sykaras N, Iacopino AM, Marker VA, Triplett RG, Woody RD. Implant materials, designs, and surface topographies: their effect on osseointegration: a literature review. *Int J Oral Maxillofac Implants*. 2000;15:675–90.
- Wennerberg A, Albrektsson T, Andersson B. Design and surface characteristics of 13 commercially available oral implant systems. *Int J Oral Maxillofac Implants*. 1993;8:622–33.
- Patel R. Clin. Biofilms and antimicrobial resistance. *Clin Orthop Relat Res*. 2005;437:41–7.
- Balaban N, Giacometti A, Cirioni O, et al. Use of the quorum-sensing inhibitor RNIII-inhibiting peptide to prevent biofilm formation in vivo by drug-resistant *Staphylococcus epidermidis*. *J Infect Dis*. 2003;187:625–30.
- Pitt WG, McBride MO, Lunceford JK, Roper RJ, Sagers RD. Ultrasonic enhancement of antibiotic action on gram-negative bacteria. *Antimicrob Agents Chemother*. 1994;38:2577–82.
- Carmen JC, Nelson JL, Beckstead BL, et al. Ultrasonic-enhanced gentamicin transport through colony biofilms of *Pseudomonas aeruginosa* and *Escherichia coli*. *J Infect Chemother*. 2004;10:193–9.
- Carmen JC, Roeder BL, Nelson JL, et al. Ultrasonically enhanced vancomycin activity against *Staphylococcus epidermidis* biofilms in vivo. *J Biomater Appl*. 2004;18:237–45.
- Caubet R, Pedarros-Caubet F, Chu M, et al. A radio frequency electric current enhances antibiotic efficacy against bacterial biofilms. *Antimicrob Agents Chemother*. 2004;48:4662–4.
- Costerton JW, Ellis B, Lam K, Johnson F, Khoury AE. Mechanism of electrical enhancement of efficacy of antibiotics in killing biofilm bacteria. *Antimicrob Agents Chemother*. 1994;38:2803–9.
- Jass J, Costerton JW, Lappin-Scott HM. The effect of electrical currents and tobramycin on *Pseudomonas aeruginosa* biofilms. *J Ind Microbiol* 1995;15:234–42.
- Jass J, Lappin-Scott HM. The efficacy of antibiotics enhanced by electrical currents against *Pseudomonas aeruginosa* biofilms. *J Antimicrob Chemother*. 1996;38:987–1000.
- Khoury AE, Lam K, Ellis B, Costerton JW. Prevention and control of bacterial infections associated with medical devices. *ASAIO J*. 1992;38(3):M174–8.
- Pickering SAW, Bayson R, Scammell BE. Electromagnetic augmentation of antibiotic efficacy in infection of orthopaedic implants. *J Bone Joint Surg*. 2003;85-B:588–93.
- Stewart PS, Wattanakaroon W, Goodrum L, Fortun SM, McLeod BR. Electrolytic generation of oxygen partially explains electrical enhancement of tobramycin efficacy against *Pseudomonas aeruginosa* biofilm. *Antimicrob Agents Chemother*. 1999;43:292–6.
- Wattanakaroon W, Stewart PS. Electrical enhancement of *Streptococcus gordonii* biofilm killing by gentamicin. *Arch Oral Biol*. 2000;45:167–71.
- Wellman N, Fortun SM, McLeod BR. Bacterial biofilms and the bioelectric effect. *Antimicrob Agents Chemother*. 1996;40:2012–4.
- Mann S. Biomimetic materials chemistry. Weinheim, Germany: Wiley-VCH; 1995.
- Mann S. In: Mann S, editor. Structure and bonding. Berlin, Heidelberg: Springer-Verlag; 1983. p. 127–74.
- Koutsoukos P, Amjad Z, Tomson MB, Nancollas GH. Crystallization of calcium phosphates. A constant composition study. *J Am Chem Soc*. 1980;102:1553–7.
- Nancollas GH. In: Mann S, Webb J, Willany RJP, editors. Biomaterialization. Weinheim, Germany: Wiley-VCH; 1989. p. 156–87.
- Amjad Z, Koutsoukos PG, Nancollas GH. The remineralization of fluoride-treated bovine enamel surfaces. *J Dent Res*. 1982;61(9):1094–8.
- Dalas E, Kallitsis JK, Koutsoukos PG. Crystallization of hydroxyapatite on polymers. *Langmuir*. 1991;7:1822–6.
- Gourdoupi N, Andreopoulou AK, Deimede V, Kallitsis JK. Novel proton-conducting polyelectrolyte composed of an aromatic polyether containing main-chain pyridine units for fuel cell applications. *Chem Mater* 2003;15(26):5044–50.
- Gourdoupi N, Papadimitriou K, Neophytides S, Kallitsis JK. New high temperature polymer electrolyte membranes. Influence of the chemical structure on their properties. *Fuel Cells*. 2008;8(3–4):200–8.
- Oikonomou EK, Pefkianakis EK, Bokias G, Kallitsis JK. Direct synthesis of amphiphilic block copolymers, consisting of poly(methyl methacrylate) and poly(sodium styrene sulfonate) blocks through atom transfer radical polymerization. *Eur Polym J*. 2008;44:1857–64.
- Amjad Z. The influence of polyphosphates, phosphonates, and poly(carboxylic acids) on the crystal growth of hydroxyapatite. *Langmuir*. 1987;3:1063–9.
- Dalas E, Kallitsis J, Koutsoukos PG. The growth of sparingly soluble salts on polymeric substrates. *Colloids Surf*. 1991;53:197–208.
- Koutsopoulos S, Kontogeorgou A, Petroheilos J, Dalas E. Calcification of porcine and human cardiac valves: testing of various inhibitors for antimaterialization. *J Mater Sci Mater Med*. 1998;9:421–4.
- Dalas E, Megas P, Tyllianakis M, Vynios D, Lambiris E. The reconstruction of large bone defects by novel functionalized polymers: an in vitro and in vivo experimental study. *J Mater Sci Lett*. 1993;12:979–81.

34. Li Y, White TJ, Lim SH. J. Low-temperature synthesis and microstructural control of titania nano-particles. *Solid State Chem.* 2004;177:1372–81.
35. Berne BJ, Pecora R. *Dynamic light scattering*. New York: Wiley; 1976.
36. Critchley I, Karginova EA, Thornsberry C. Prevalence of biofilm production in recent clinical isolates of *Staphylococcus aureus*, *Staphylococcus epidermidis* and *Pseudomonas aeruginosa*. In: 42nd interscience conference on antimicrobial agents and chemotherapy. Abstract No. B-269, 2002.
37. Gallo J, Kolar M, Florschütz A, Novotny R, Pantucek R, Kesselova M. In vitro testing of vancomycin—gentamicin loaded bone cement to prevent prosthetic joint infection. *Biomed Papers.* 2005;149(1):153–8.
38. JCPDS, File No. 24-0033.
39. Koutsopoulos S, Paschalakis PC, Dalas E. The calcification of elastin in vitro. *Langmuir.* 1994;10:2423–8.
40. Verma A, Uzun O, Hu Y, Han HS, Watson N, Chen S, Irvine DJ, Stellacci F. Surface-structure-regulated cell-membrane penetration by monolayer-protected nanoparticles. *Nat Mater.* 2008;7: 588–95.
41. Kumar A, Vemula PK, Ajayan PM, John G. Silver-nanoparticle-embedded antimicrobial paints based on vegetable oil. *Nat Mater.* 2008;7:236–41.
42. Kenawy ER, Mahmoud YAG. Biologically active polymers, 6: synthesis and antimicrobial activity of some linear copolymers with quaternary ammonium and phosphonium groups. *Macromol Biosci.* 2003;3(2):107–116.
43. Koutsopoulos S, Dalas E. The calcification of fibrin in vitro. *J Cryst Growth.* 2000;216:450–8.
44. Koutsoukos PG, Nancollas GH. The mineralization of collagen in vitro. *Colloids Surf.* 1987;28:95–108.
45. Dalas E. Crystallization of sparingly soluble salts on functionalized polymers. *J Mater Chem.* 1991;1:473–4.
46. Chrissanthopoulos A, Malkaj P, Dalas E. Calcium phosphate crystallization on polyglycine, polytyrosine and polymethionine. *Mater Lett.* 2006;60:3874–8.
47. Dalas E, Chrissanthopoulos A. The overgrowth of hydroxyapatite on new functionalized polymers. *J Cryst Growth.* 2003;255: 163–9.
48. Kanakis J, Chrissanthopoulos A, Tzanetos NP, Kallitsis JK, Dalas E. Crystallization of hydroxyapatite on oxadiazole-based homopolymers. *Cryst Growth Des.* 2006;6:1547–52.
49. Neut D, Van Der Mei HC, Bulstra SK, Busscher HJ. The role of small-colony variants in failure to diagnose and treat biofilm infections in orthopedics. *Acta Orthopaedica.* 2007;78(3): 299–308.
50. Campoccia D, Montanaro L, Arciola CR. The significance of infection related to orthopedic devices and issues of antibiotic resistance. *Biomaterials.* 2006;27:2331–9.
51. Oldenburg SJ, Averitt RD, Westcott SL, Halas NJ. Nanoengineering of optical resonances. *Chem Phys Lett.* 1998;288:243–7.
52. Hirsch LR, Stafford RJ, Bankson JA, Sershen SR, Rivera B, Price RE, Hazle JD, Halas NJ, West JL. Nanoshell-mediated near-infrared thermal therapy of tumors under magnetic resonance guidance. *PNAS.* 2003;100(23):13549–54.
53. O'Neal DP, Hirsch LR, Halas NJ, Payne JD, West JL. Photo-thermal tumor ablation in mice using near infrared-absorbing nanoparticles. *Cancer Lett.* 2004;209:171–6.